BIOLOGICAL CRYSTALLOGRAPHY

ISSN 1399-0047

A structural view of the dissociation of *Escherichia coli* tryptophanase

Keren Green,[a,b]‡ Nasrin Qasim,[a,b]‡ Garik Gdaelvsky,[b] Anna Kogan,[a,b] Yehuda Goldgur,[c] Abraham H. Parola,[b,d] Ofra Lotan[a] and Orna Almog[a]*

[a]Department of Clinical Biochemistry and Pharmacology, Ben-Gurion University of the Negev, PO Box 105, Beer Sheva 84105, Israel, [b]Department of Chemistry, Ben-Gurion University of the Negev, PO Box 105, Beer Sheva 84105, Israel, [c]Structural Biology Program, Memorial Sloan Kettering Cancer Center, 1275 York Avenue, New York, NY 10065, USA, and [d]Faculty of Arts and Science, New York University Shanghai (NYUSH), Shanghai 200122, People's Republic of China. *Correspondence e-mail: almogo@bgu.ac.il

Received 19 August 2015
Accepted 25 September 2015

Edited by Z. S. Derewenda, University of Virginia, USA

‡ These authors contributed equally.

Keywords: PLP-dependent enzyme; closed conformation; cold dissociation; hydrophobic interactions; crystal structure.

PDB reference: tryptophanase, 5d8g

Supporting information: this article has supporting information at journals.iucr.org/d

Tryptophanase (Trpase) is a pyridoxal 5′-phosphate (PLP)-dependent homotetrameric enzyme which catalyzes the degradation of L-tryptophan. Trpase is also known for its cold lability, which is a reversible loss of activity at low temperature (2°C) that is associated with the dissociation of the tetramer. *Escherichia coli* Trpase dissociates into dimers, while *Proteus vulgaris* Trpase dissociates into monomers. As such, this enzyme is an appropriate model to study the protein–protein interactions and quaternary structure of proteins. The aim of the present study was to understand the differences in the mode of dissociation between the *E. coli* and *P. vulgaris* Trpases. In particular, the effect of mutations along the molecular axes of homotetrameric Trpase on its dissociation was studied. To answer this question, two groups of mutants of the *E. coli* enzyme were created to resemble the amino-acid sequence of *P. vulgaris* Trpase. In one group, residues 15 and 59 that are located along the molecular axis *R* (also termed the noncatalytic axis) were mutated. The second group included a mutation at position 298, located along the molecular axis *Q* (also termed the catalytic axis). Replacing amino-acid residues along the *R* axis resulted in dissociation of the tetramers into monomers, similar to the *P. vulgaris* Trpase, while replacing amino-acid residues along the *Q* axis resulted in dissociation into dimers only. The crystal structure of the V59M mutant of *E. coli* Trpase was also determined in its apo form and was found to be similar to that of the wild type. This study suggests that in *E. coli* Trpase hydrophobic interactions along the *R* axis hold the two monomers together more strongly, preventing the dissociation of the dimers into monomers. Mutation of position 298 along the *Q* axis to a charged residue resulted in tetramers that are less susceptible to dissociation. Thus, the results indicate that dissociation of *E. coli* Trpase into dimers occurs along the molecular *Q* axis.

1. Introduction

Escherichia coli tryptophanase (tryptophan indole-lyase; Trpase; EC 4.1.99.1) is a bacterial pyridoxal 5′-phosphate (PLP)-dependent enzyme that catalyzes the degradation of L-tryptophan to pyruvate, ammonia and indole. Trpase consists of four identical subunits (∼52 kDa per monomer), each of which binds one molecule of PLP, which is essential for the enzymatic activity. The tetramer possesses D_2 symmetry; therefore, it is a dimer of dimers with two different dimeric interfaces along two molecular axes *R* and *Q* (Fig. 1; Isupov *et al.*, 1998; Högberg-Raibaud *et al.*, 1975; Suelter & Snell, 1977; Suelter *et al.*, 1976*a*; Toraya *et al.*, 1976; Phillips, 1989; Phillips *et al.*, 1990, 2002, 2003). Dissociation along the *R* axis results in *AB* and *CD* dimers, and dissociation along the *Q* axis results in *AC* and *BD* dimers (Fig. 2).

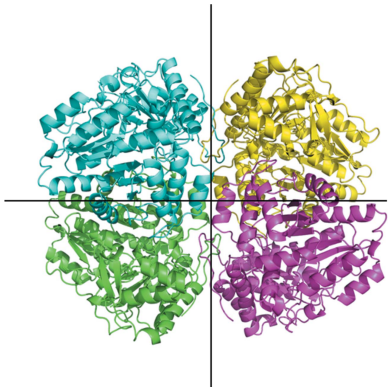

Trpases are also known for their cold lability, which includes loss of activity and dissociation following incubation at 2°C for several hours. The catalytic activity may be restored by incubating the enzyme at 20 or 37°C in the presence of PLP for several hours (Erez, Gdalevsky *et al.*, 1998; Erez, Phillips *et al.*, 1998). Using kinetic spectrophotometric methods and size-exclusion chromatography, we have previously shown that the inactivation process is linked to release of the PLP molecule and to dissociation of the tetrameric form of Trpase (Erez *et al.*, 2002). It has also previously been shown that *E. coli* Trpase dissociates into dimers, while *Proteus vulgaris* Trpase dissociates into monomers (Kogan *et al.*, 2009). The present study was designed to understand this difference between the two Trpases and to unravel which molecular axis the dissociation of *E. coli* Trpase into dimers takes place along.

Three crystal structures of bacterial Trpases are available. One is of *P. vulgaris* Trpase, which shares 51% identity in its amino-acid sequence with the *E. coli* enzyme, in its holo form (PLP-bound; Isupov *et al.*, 1998). The other two crystal structures are of *E. coli* Trpase in the apo form (PLP-depleted), one determined by Ku *et al.* (2006) (referred to here as the apoI structure) and the other determined by Tsesin *et al.* (2007) (referred to here as the apoII structure). Recently, a new crystal structure of *E. coli* Trpase in a 'semi-holo' form has been reported (Kogan *et al.*, 2015).

The three-dimensional structure of all Trpases consists of two domains: the large domain and the small domain. Both domains are built around β-sheets with flanking α-helices. The large and small domains can undergo significant movement with respect to each other upon PLP binding, going from a closed conformation for holo Trpase to a wide-open conformation for apo Trpase. This conformational change has also been reported for other related PLP-binding enzymes such as tyrosine phenol-lyase (TPL; Milić *et al.*, 2006) and aspartate aminotransferase (Almog *et al.*, 2008).

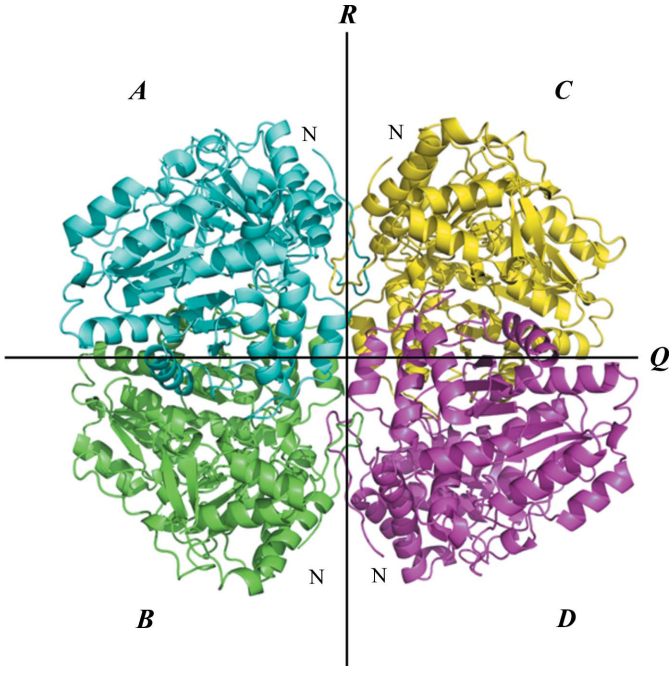

Figure 1
The tetrameric crystal structure of *P. vulgaris* Trpase (PDB entry 1ax4), in which each chain is shown in a different colour and the molecular axes *R* and *Q* are shown as black lines.

We used the known crystal structures of Trpases to design rational mutants. The new mutants were aimed at understanding the dissociation process of the tetrameric form of the enzyme. The mutation sites chosen are located at different interfaces of the tetramer: along the *R* axis and the *Q* axis (Fig. 2; Isupov *et al.*, 1998). Amino acids on the surface and along the *R* axis that differ between the Trpases were replaced to resemble those of the *P. vulgaris* enzyme. Along the *Q* axis one amino-acid residue (298) was replaced to study the effect of hydrophobicity and size on the dissociation of the enzyme. With the aim of a more holistic understanding of the effect of the mutations, we carried out a three-dimensional structure analysis of all Trpases. Based on our results, we concluded that the dissociation of *E. coli* Trpase occurs along the *Q* axis, resulting in *AC* and *BD* dimers. This is owing to stronger hydrophobic interactions between the *A* and *C* monomers (and equivalently the *B* and *D* monomers), which in the case of *E. coli* Trpase do not further dissociate into monomers.

2. Experimental procedures

2.1. Materials

S-(*o*-Nitrophenyl)-L-cysteine (SOPC) was synthesized as described previously (Phillips *et al.*, 1989) and was used as a substrate for activity measurements. PLP, Tricine, L-tryptophan, β-mercaptoethanol, protamine sulfate, ampicillin, buffers and ammonium sulfate were purchased from Sigma. Other chemicals, obtained from various commercial suppliers, were of pure or extra pure grade.

2.2. Mutation

The pMD6 plasmid carrying the wild-type Trpase gene was a gift from Professor R. Phillips, University of Georgia, USA. Mutation sites were chosen following sequence comparison of the *E. coli* and *P. vulgaris* Trpases. Mutagenesis was carried out using the QuikChange Lightning Site-Directed Mutagenesis Kit (Agilent Technologies) according to the manufacturer's manual. Mutation sites were confirmed by sequencing the entire gene.

2.3. Purification of *E. coli* Trpase variants

Wild-type Trpase and its variants were isolated from *E. coli* SVS 370 cells containing the *tnaA* gene on plasmid pMD6 by a previously described procedure (Phillips & Gollnick, 1989). Additional purification was achieved by anion-exchange chromatography on DEAE-Sephadex A-50 or DEAE-Sepharose 4B-CL and size-exclusion chromatography on Sephacryl S-300 HR (Erez, Gdalevsky *et al.*, 1998; Kogan *et al.*, 2004). The details of purification are described in Kogan *et al.* (2009).

2.4. Enzymatic activity measurements

Activity was measured by a spectrophotometric method using the chromogenic substrate analogue *S*-(*o*-nitrophenyl)-L-cysteine (SOPC), as described in Suelter *et al.* (1976*a*,*b*); see also Kogan *et al.* (2009).

2.5. Production of the apo forms of Trpases

Apo enzymes were prepared by overnight dialysis of the holo enzyme in the cold against 0.25 *M* sodium phosphate buffer containing 0.1 *M* L-alanine pH 7.0 (Erez, Gdalevsky *et al.*, 1998; Erez *et al.*, 2002; Erez, Phillips *et al.*, 1998).

2.6. Crystallization of the V59M mutant

Crystallization experiments were carried out at 20°C and were set up using the hanging-drop vapour-diffusion method with siliconized cover slips and Linbro 24-well tissue-culture plates. Droplets ranging in size from 5 to 10 µl were prepared by mixing equal volumes of the protein solution and reservoir solution and were equilibrated against 1.0 ml reservoir solution at room temperature (20°C). The protein concentration of the V59M variant was 30–50 mg ml^{-1} in 50 m*M* Tris, 100 m*M* KCl pH 7.5, 2 m*M* EDTA, 5 m*M* β-mercaptoethanol. The protein solution was mixed with reservoir solution consisting of 30%(*w*/*v*) PEG 400, 100 m*M* HEPES pH 7.5, 200 m*M* $MgCl_2$, 5 m*M* β-mercaptoethanol (Kogan *et al.*, 2004).

2.7. Data collection and structure determination

Crystals were transferred to Paratone oil (Hampton Research) and excess liquid was removed, followed by cooling in liquid nitrogen. A diffraction data set for the apo V59M mutant was collected at low temperature (100 K) using an R-AXIS IV electronic area detector and a Rigaku RU-200 HB generator. The unit-cell parameters and crystal orientation

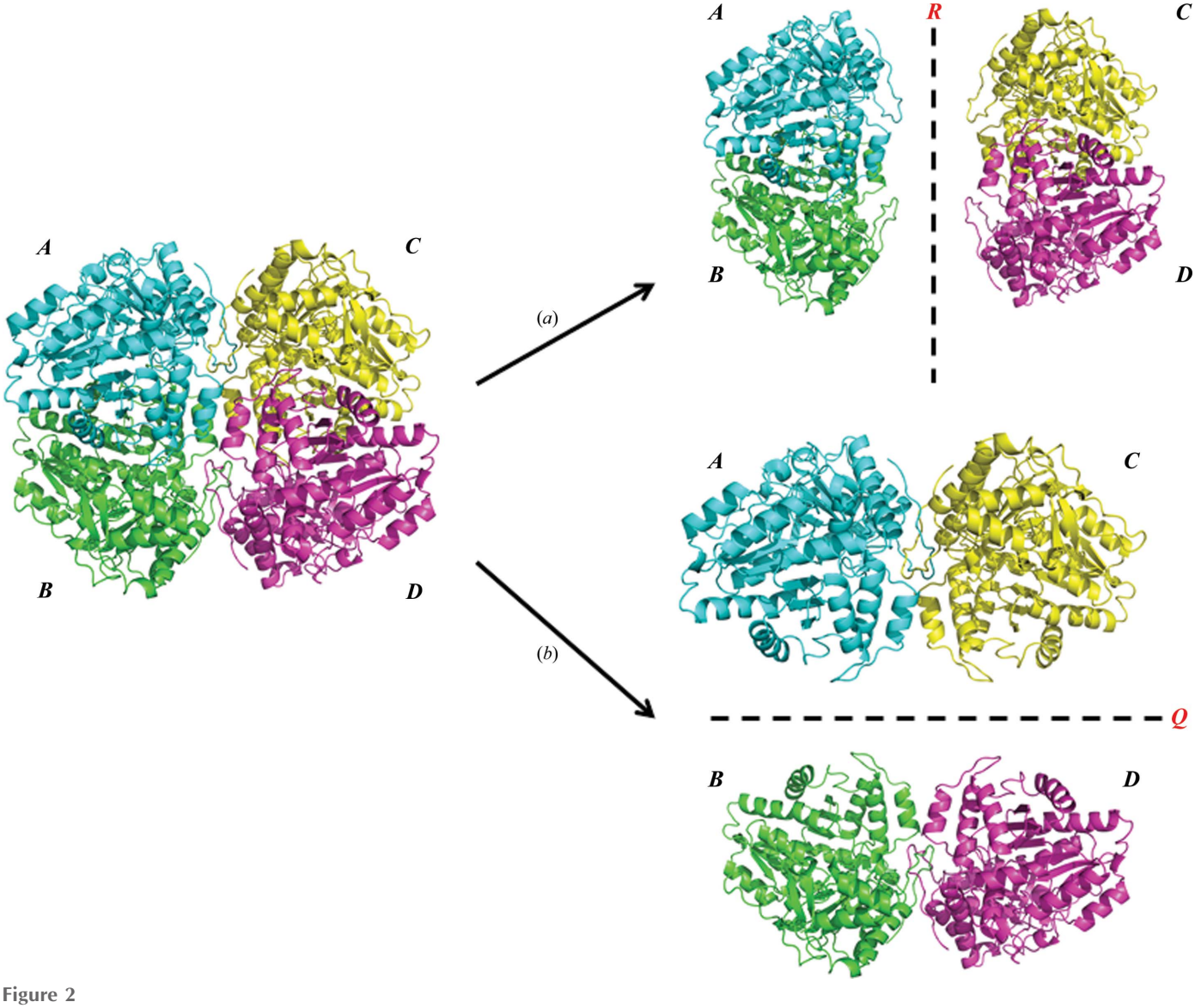

Figure 2
A schematic representation of the two possible mechanisms of dissociation of Trpase. (*a*) Dissociation along the *R* axis results in *AB* and *CD* dimers. (*b*) Dissociation along the *Q* axis results in *AC* and *BD* dimers.

Table 1
Data-collection and refinement statistics for the V59M mutant.

Wavelength (Å)	1.5418
Resolution range (Å)	49.2–1.9
Space group	*F*222
Unit-cell parameters (Å)	a = 118.3, b = 120.3, c = 171.7
Multiplicity	6.6
Completeness (%)	99.0 (96.1)
R_{merge} (%)	14.9
$\langle I/\sigma(I)\rangle$	10.2
Subunits in asymmetric unit	1
Total reflections	45940
Reflections in working set	21182 (3285)
Reflections in test set	2449
R_{work}/R_{free}	0.174/0.214
No. of atoms	
Total	4052
Protein	3730
Water	421
Ion	6
Mean B value (Å^2)	25.3
R.m.s. deviations	
Bond lengths (Å)	0.022
Bond angles (°)	1.970

were determined and integration of reflection intensities was performed using the *HKL*-2000 package (Otwinowski & Minor, 1997). The coordinates of apo Trpase (PDB entry 2oqx; Tsesin *et al.*, 2007) were used as the search model and the structure was refined using *REFMAC*5 (Murshudov *et al.*, 2011); manual model rebuilding was performed with the graphics program *Coot*. The refined coordinates of the structure were deposited in the Protein Data Bank (PDB entry 5d8g). Data-collection and refinement statistics are given in Table 1.

3. Results

3.1. Mutations along the *R* axis

The sites for substitution along the *R* axis were chosen by comparing the amino-acid sequence of *E. coli* Trpase with that of *P. vulgaris* Trpase. Amino acids at the interface region of each monomer were identified using structural comparison of the three crystal structures of Trpase. The rationale for this was that *P. vulgaris* Trpase dissociates into monomers, while the *E. coli* enzyme dissociates into dimers only. Analysis of the interface in both Trpases (from *E. coli* and *P. vulgaris*) revealed that the β-sheet located at the core of the tetramer is not exposed to the solvent. Furthermore, the four β-strands are structurally similar but differ in their amino-acid content. Met57, Met13 and Val14 of *P. vulgaris* Trpase are replaced by Val59, Val15 and Ile16 in *E. coli* Trpase. The two valine residues and the isoleucine residue in the *E. coli* enzyme are more hydrophobic than the corresponding two methionine residues and the valine residue in the *P. vulgaris* enzyme (Black & Mould, 1991). Based on this analysis, we studied the role of these amino acids on the mode of dissociation.

Three mutants were prepared, V15M, V59M and the double mutant V15M/V59M, to resemble *P. vulgaris* Trpase. The I16V mutant was toxic and we were unable to overexpress it. The degree of dissociation and the activity of the three *E. coli*

Table 2
Activity and dissociation of the *E. coli* Trpase holo-form mutants (mutations along the *R* axis).

Mutant	Specific activity at 25°C (units per milligram of protein)	Dissociation to dimers at 25°C (%)	Dissociation to dimers at 2°C (%)
Holo Trpase WT	45 ± 2.5	≤3	29 ± 2
Holo Trpase V59M	25 ± 5.0	6 ± 2	63 ± 2
Holo Trpase V15M	12 ± 2.0	15 ± 3	39 ± 5
Holo Trpase V59M/V15M	6 ± 3.0†	76 ± 4	33 ± 3 and 43 ± 2 (monomers)

† These measurements were taken for a partially purified mutant.

Table 3
Dissociation of the *E. coli* Trpase apo-form mutants (mutations along the *R* axis).

Mutant	Dissociation to dimers at 25°C (%)	Dissociation to dimers at 2°C (%)
Apo Trpase WT	60 ± 5	80 ± 6
Apo Trpase V59M	67 ± 3	80 ± 2
Apo Trpase V15M	96 ± 1	85 ± 3 (monomers)
Apo Trpase V59M/V15M	81 ± 2	32 ± 2 and 55 ± 3 (monomers)

mutants in their holo form (active, PLP-bound) were determined and are summarized in Table 2. Mutations along the *R* axis induced the following activity and dissociation changes. (i) Each of them decreased the specific activity measured at 25°C. (ii) A different extent of effect on the activity was obtained with each kind of mutation. (iii) The double mutant exhibited a negligible enzymatic activity, reflecting a synergistic decreasing effect. (iv) The degree of dissociation of all three mutants measured at 25°C increased. (v) The extent of the increase in dissociation correlated with the extent of the decline in activity. Namely, the higher the degree of dissociation, the deeper the decline in activity. It should be noted that while at 25°C dissociation into dimers only occurs, at 2°C the double mutant is shown here for the first time to dissociate all the way into monomers (Table 2).

In contrast to most enzymes, which are more stable at low temperatures, Trpase is known for its cold lability; namely, a higher degree of dissociation at low temperatures. Indeed, mutants along the *R* axis resulted in an increased extent of dissociation at 2°C compared with 25°C.

Table 3 shows the degree of dissociation for the wild type (WT) and for the new mutants of Trpase, all in their apo forms. While the holo (PLP-bound) form represents the active form of the enzyme, the apo (PLP-depleted) form represents the nonactive form (usually found at 2°C) (Kogan *et al.*, 2009). The data summarized in Table 3 are for the *E. coli* mutants in their apo forms, which were generated by overnight dialysis of the isolated active forms. In comparison with the holo-form mutants (Table 2), the degree of dissociation of all apo-form mutants increased dramatically (to about 70%) even at 25°C, indicating that PLP plays a crucial role in holding the tetrameric quaternary structure together. Interestingly, while the dissociation at 25°C is only to dimers, at low temperature

Table 4
Activity and dissociation of the *E. coli* Trpase holo-form mutants (mutations along the *Q* axis).

Mutant	Specific activity at 25°C (units per milligram of protein)	Dissociation to dimers at 25°C (%)	Dissociation to dimers at 2°C (%)
Holo Trpase WT	42.7 ± 2.5	≤3	24 ± 2
Holo Trpase C298S	37 ± 3	5 ± 1	64 ± 5
Holo Trpase C298A	12 ± 2	82 ± 3	80 ± 5
Holo Trpase C298D	0.3	8 + 1	1

(2°C) dissociation of the apo form is enhanced and monomers are found for the V15M variant as well as for the double mutant V15M/V59M, indicating the role of hydrophobic interaction in the stability of *E. coli* Trpase.

3.2. Mutations along the *Q* axis

Previous biochemical (Phillips & Gollnick, 1989) and structural (Kogan *et al.*, 2009) studies have shown that, although not part of the active site, amino acid 298 affects the activity of the enzyme, probably owing to an interaction with Arg101, which is part of the active site of the adjacent monomer. It has also been shown that mutation at this site increases the degree of dissociation to dimers at 2°C (cold lability), probably owing to excessive release of PLP (Kogan *et al.*, 2009).

In order to understand whether this site plays a role in holding the two monomers *A* and *B* or *C* and *D* together as a dimer (Fig. 1), preventing dissociation into monomers, we mutated it to alanine and to aspartate (C298A and C298D). These mutants complement our previously studied mutant C298S (Kogan *et al.*, 2009).

We hypothesized that since the alanine residue is more hydrophobic than the wild-type cysteine, the degree of dissociation would increase dramatically, to the extent of resulting in monomers, and that in the case of the aspartate residue, which exhibits a negatively charged side chain, the degree of dissociation would decrease dramatically. The results summarized in Table 4 indicate that the C298A and C298D mutants resulted in decreased activity of the holo form of the enzyme at 25°C that did not correlate with the degree of dissociation. The holo form of the C298D mutant was almost inactive despite a low degree of dissociation. Mutating Cys298 to the similarly hydrophobic serine residue had a small effect on the activity and on the dissociation at 25°C compared with the WT, and had no effect on the crystal structure. The similar stability (low dissociation) of the C298D apo mutant at 25 and 2°C (Table 5) implies that it is not PLP that promotes the interaction between the monomers. Absorption spectra of the residue 298 variants in their holo form at 25°C (data not shown) suggest that the cofactor PLP is present at the active site in all of them, including the non-active C298D. Structural modelling of the aspartate residue at position 298 replacing a cysteine suggested that a stronger ionic bond is created with Arg103 (see §3.4), preventing the correct positioning of PLP in the active site of the adjacent monomer (Fig. 3).

Table 5
Dissociation of the *E. coli* Trpase apo-form mutants (mutations along the *Q* axis).

Mutant	Dissociation to dimers at 25°C (%)	Dissociation to dimers at 2°C (%)
Apo Trpase WT	70 ± 5	87 ± 3
Apo Trpase C298S	>80	88 ± 1
Apo Trpase C298A	79 ± 9	90 ± 2
Apo Trpase C298D	19 ± 1	25 ± 2

3.3. The crystal structure of the Trpase V59M mutant (mutation along the *R* axis)

We determined the crystal structure of the V59M mutant in its apo form and compared it with the WT Trpase crystal structure (Tsesin *et al.*, 2007) (Fig. 4). The two crystal structures were found to be identical, with the same crystallization conditions, space group and unit cell. The r.m.s. deviation between the two structures was found to be 0.129 Å for 434 C^{α} atoms. The mutation site (residue 59) could be fitted clearly to the electron-density map (Fig. 5). This result is in agreement with the degree of dissociation measured for the V59M mutant in its apo form compared with the WT. Moreover, no monomers could be detected for the V59M mutant at either 25 or 2°C. Interestingly, despite the similar structures of the WT and the V59M mutant, the mutation does exhibit an effect on the activity and the dissociation of the holo form (Table 2).

We further compared the crystal structure of the V59M mutant with the crystal structures of three Trpases: (i) apoI in the closed conformation (PDB entry 2c44; Ku *et al.*, 2006), (ii) apoII in the wide-open conformation (PDB entry 2oqx; Tsesin *et al.*, 2007) and (iii) holo Trpase isolated from *P. vulgaris* (Isupov *et al.*, 1998). The r.m.s. deviations were found to be 2.26 Å (for 434 atoms), 0.129 Å (for 410 atoms) and 1.866 Å (for 429 atoms), respectively. The side chain of position 59 in all four crystal structures is depicted in Fig. 5. The orientation

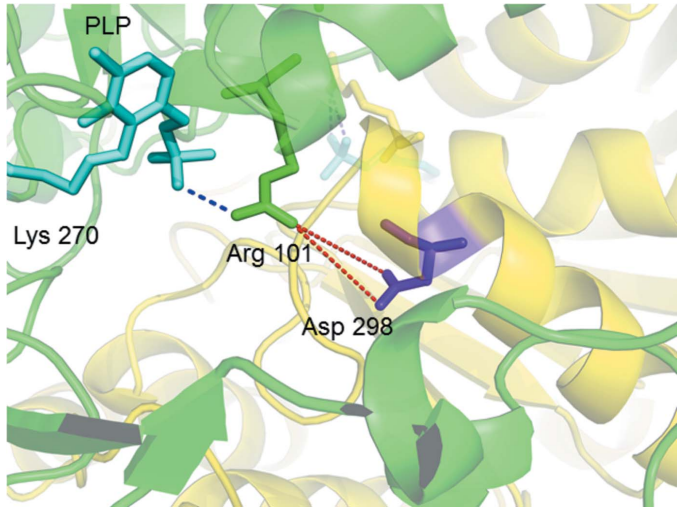

Figure 3
A structural model of *E. coli* Trpase in which Cys298 is replaced by Asp (shown in purple), suggesting that Asp creates a stronger ionic bond with Arg101 (shown as green), preventing the correct positioning of PLP (shown in cyan) in the active site of the adjacent molecule.

of the valine residue of both apo forms (apoI and apoII) is identical, while the orientation of the methionine residue of *P. vulgaris* Trpase and of the apo V59M mutant is only similar.

3.4. Modelling of the structures of mutants along the *Q* axis

In order to understand the unique stability of the C298D mutant (Tables 4 and 5), we performed *in silico* modelling. We found that the side chain of Arg103 also occupies an identical position in the apoI and holo Trpase (*P. vulgaris*) structures, while that of the side chain of Arg103 in the apoII (and the V59M) structure differs, being positioned about 9 Å away (Fig. 6) and indicating the possible movement of this side chain to create a hydrogen bond to the aspartate residue of the adjacent molecule (*A* and *B*).

The different positions of the Arg103 side chain in the apoI and apoII structures may be related to the closed conformation of the apoI (and *P. vulgaris* Trpase) structures compared with the open conformation of the apoII structure. In the apoI structure two sulfate anions are found in the active-site region, probably originating from the crystallization solution used. One of the sulfate ions (PDB entry 2c44) is positioned at the same site as the phosphate of the PLP cofactor in *P. vulgaris* Trpase. The second sulfate is 4.3 Å away, in the substrate-site region (Fig. 7). These anions render the active-site region negatively charged, which results in 'movement' of the small domain towards the large domain of *E. coli* Trpase, resulting in the closed conformation. The apoII structure was found with no sulfate ions bound to it and therefore showed a wide-open conformation. In the holo Trpase from *P. vulgaris* the PLP cofactor includes only one phosphate and as such it is found in mid-transition between the wide-open apoII structure and the tightly closed apoI structure.

An additional significant difference between the holo Trpase and apoI structures compared with the apoII (and V59M) structure was found in the conformation of the loop composed of residues 295–310. This loop includes the mutation site at residue 298 (Fig. 8). The loop is found in two

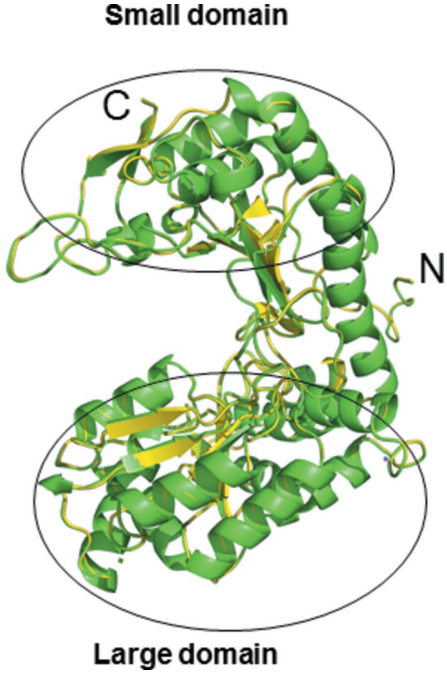

Figure 4
The crystal structure of the V59M mutant of Trpase (shown in green) in its apo form superimposed on the crystal structure of WT Trpase (shown in yellow). The large and the small domains are indicated.

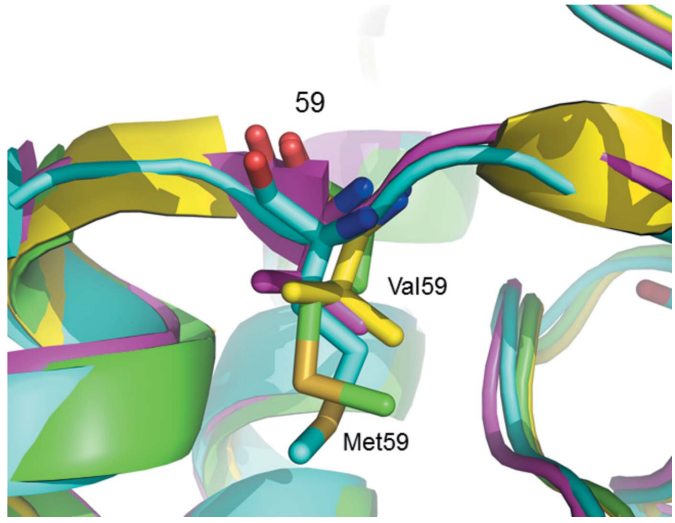

Figure 5
The side-chain orientation of residue 59 in four Trpases. The Val side chains in the apoI structure (PDB entry 2c44, shown in magenta) and the apoII structure (PDB entry 2oqx, shown in yellow) exhibit identical orientations. The Met side chains in holo *P. vulgaris* Trpase (shown in cyan) and the V59M mutant (shown in green) exhibit a somewhat different orientation, which is possibly responsible for the differences in activity between the V59M mutant and WT Trpases in the holo form.

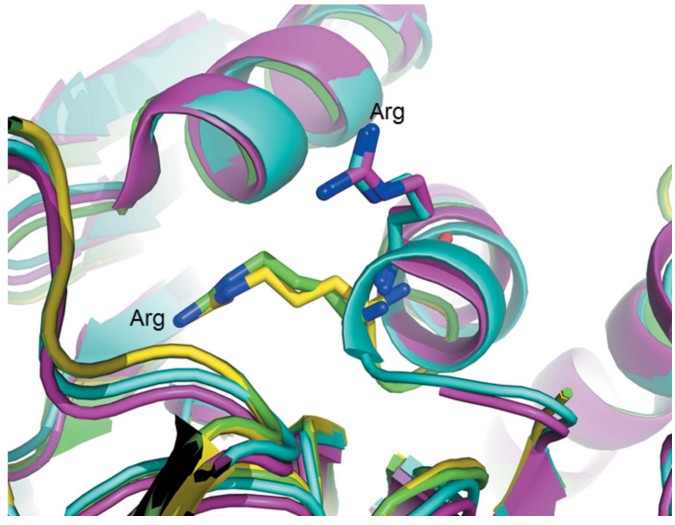

Figure 6
The orientation of the side chains of the equivalent Arg residues (Arg101 in *P. vulgaris* Trpase and Arg103 in *E. coli* Trpase). The Arg side chains in the apoI (shown in magenta) and holo Trpase (shown in cyan) structures occupy an identical position. In the apoII (shown in yellow) and V59M mutant structures the side chain of Arg is differently positioned about 9 Å away. This may indicate possible movement of this side chain to create a hydrogen bond to the Asp residue of the adjacent monomer.

conformations: one is found in the enzymes in the closed conformation (apoI and holo) and the other is found in those in the wide-open conformation (apoII). This suggests that the loop composed of residues 295–310 is highly flexible and may be involved in the transition between the closed and open conformations as well as in adjusting the monomer–monomer interaction, *i.e.* *A* and *B* *versus* *C* and *D* (see Fig. 2).

4. Discussion

A central conclusion of the present study is that the dissociation of *E. coli* Trpase occurs along the *Q* axis of the molecule and results in *AC* and *BD* dimers (Fig. 2). This conclusion is based on the following points.

(i) It is shown here for the first time for *E. coli* Trpase that mutating residues 15 and 59 along the *R* axis to resemble those in *P. vulgaris* Trpase led to dissociation of the tetrameric form into monomers. This suggests that in *E. coli* Trpase dissociation occurs along the *Q* axis and results in dimers (*AC* and *BD*). Hydrophobic interactions at the interface between each two monomers (*A* and *C* and *B* and *D*) hold them together as dimers. Namely, a more hydrophobic core in the region of the interface presumably leads to a higher stability of the dimeric structure of *E. coli* Trpase compared with *P. vulgaris* Trpase. Dimers of *E. coli* Trpase further dissociate into monomers when residues on this interface (such as 15 and 59) are replaced.

(ii) The suggested mode of dissociation is further supported by mutants along the *Q* axis, which did not result in dissociation into monomers at all (position 298).

(iii) The activity of the holo enzyme has previously been reported to be affected by mutating cysteine 298, located on the *Q* axis, to serine (Phillips & Gollnick, 1989). It is conceivable that this occurs owing to a conformational change of the loop composed of residues 290–310 (Isupov *et al.*, 1998; Kogan *et al.*, 2009). Our group has previously shown that Cys298 of monomer *A* interacts with Arg103 of the adjacent monomer (*B*; Fig. 3; Kogan *et al.*, 2009). In the present study we further mutated Cys298 to Ala and Asp, which differ in size and hydrophobicity, to better understand the role of the above interaction in the dissociation of *E. coli* Trpase. Based on the finding that no monomers were obtained even when we replaced Cys298 by alanine, which dramatically affected the degree of dissociation into dimers (even at 25°C; Table 4), we conclude that residue 298 is not involved in the dissociation of Trpase into monomers.

(iv) An additional central finding was that residue 298 stabilized the tetrameric form when replaced by a hydrophilic side chain (*D*). It is conceivable that since aspartate has a more polar or hydrophilic side chain than cysteine the interaction between monomers *A* and *B* in the C298D mutant is stronger, preventing dissociation into dimers. In contrast, mutations along the *R* axis did result in monomers, suggesting that the cascade of events of the dissociation process of Trpases starts with dissociation into *AC* and *BD* dimers and only then dissociation into monomers.

(v) Analysing the crystal structures of all Trpases indicated that they exhibit a highly similar overall structure. Differences were found between the closed conformation (apoI and holo) and the wide-open conformation (apoII and V59M). This is probably owing to the presence of ions in the regulatory site (cofactor-binding site) or in the active site (substrate-binding site).

Understanding the mechanism of the dissociation/association processes of multimeric enzymes at the molecular level will enable such enzymes to be modified into more stable forms and accelerate their use as industrial catalysts. While in

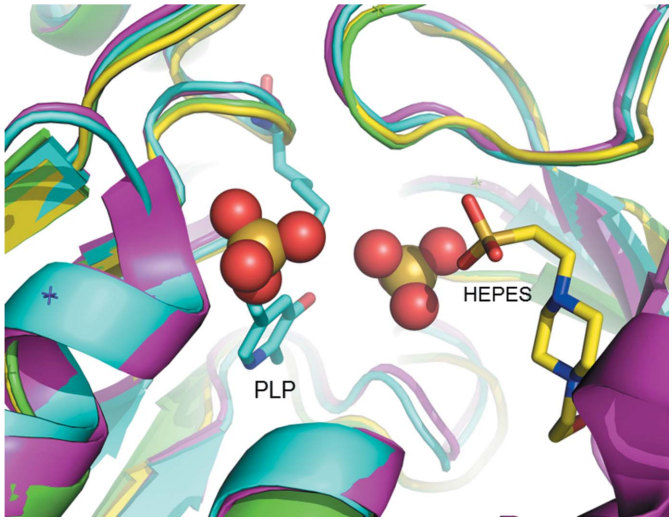

Figure 7
The active-site region of Trpase. In the apoI structure (PDB entry 2c44) two sulfate anions are shown as orange and red spheres, one positioned at the same site as the phosphate ion of the cofactor PLP (shown in cyan) and the other 4.3 Å away in the substrate-site region.

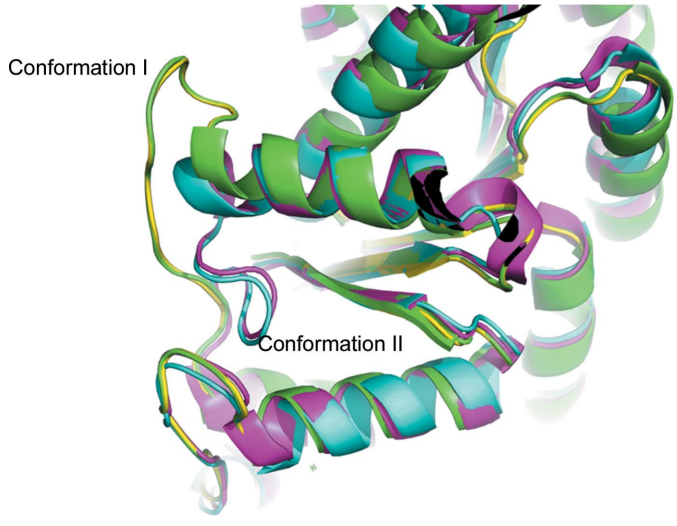

Figure 8
The conformation of the Trpase loop composed of residues 295–310. The loop exhibits two different conformations. The loops of the apoI (PLP-depleted) and holo Trpase (PLP-bound) structures exhibit the same conformation and both proteins display a closed structure. The loops of the apoII and V59M structures exhibit the same conformation and both proteins display a wide-open structure. This suggests that the 295–310 loop is highly flexible and may be involved in the transition between the closed and open Trpase structures.

most monomeric enzymes the first step of their inactivation involves changes in the tertiary structure, the first step in the inactivation of multimeric enzymes is, in many cases, the dissociation of the subunits of the enzyme or the loss of their correct assembled structure. Studies of the dissociation of multimeric enzymes are mainly based on spectroscopy. The peculiar aspect of the present study, in which we used the multimeric Trpase as a model system to study the molecular coordinates of dissociation reactions, is the fact that although the tools utilized are stationary they enabled dynamic ultrafast processes to be revealed. The study suggests a structural view of protein–protein interaction and of the mechanism of dissociation at the molecular level.

Acknowledgements

The financial support of the James Franck Center for Laser–Matter Interaction (to AHP) and of the Edmund Safra Center for Functional Biopolymers (to AHP) and an NYU Shanghai research grant to AHP are gratefully acknowledged.

References

Almog, O., Kogan, A., de Leeuw, M., Gdalevsky, G. Y., Cohen-Luria, R. & Parola, A. H. (2008). *Biopolymers*, **89**, 354–359.
Black, S. D. & Mould, D. R. (1991). *Anal. Biochem.* **193**, 72–82.
Erez, T., Gdalevsky, G. Y., Hariharan, C., Pines, D., Pines, E., Phillips, R. S., Cohen-Luria, R. & Parola, A. H. (2002). *Biochim. Biophys. Acta*, **1594**, 335–340.
Erez, T., Gdalevsky, G., Torchinsky, Y. M., Phillips, R. S. & Parola, A. H. (1998). *Biochim. Biophys. Acta*, **1384**, 365–372.
Erez, T., Phillips, R. S. & Parola, A. H. (1998). *FEBS Lett.* **433**, 279–282.
Högberg-Raibaud, A., Raibaud, O. & Goldberg, M. E. (1975). *J. Biol. Chem.* **250**, 3352–3358.
Isupov, M. N., Antson, A. A., Dodson, E. J., Dodson, G. G., Dementieva, I. S., Zakomirdina, L. N., Wilson, K. S., Dauter, Z., Lebedev, A. A. & Harutyunyan, E. H. (1998). *J. Mol. Biol.* **276**, 603–623.
Kogan, A., Gdalevsky, G. Y., Cohen-Luria, R., Goldgur, Y., Phillips, R. S., Parola, A. H. & Almog, O. (2009). *BMC Struct. Biol.* **9**, 65.
Kogan, A., Gdalevsky, G. Y., Cohen-Luria, R., Parola, A. H. & Goldgur, Y. (2004). *Acta Cryst.* D**60**, 2073–2075.
Kogan, A., Raznov, L., Gdalevsky, G. Y., Cohen-Luria, R., Almog, O., Parola, A. H. & Goldgur, Y. (2015). *Acta Cryst.* F**71**, 286–290.
Ku, S.-Y., Yip, P. & Howell, P. L. (2006). *Acta Cryst.* D**62**, 814–823.
Milić, D., Matković-Čalogović, D., Demidkina, T. V., Kulikova, V. V., Sinitzina, N. I. & Antson, A. A. (2006). *Biochemistry*, **45**, 7544–7552.
Murshudov, G. N., Skubák, P., Lebedev, A. A., Pannu, N. S., Steiner, R. A., Nicholls, R. A., Winn, M. D., Long, F. & Vagin, A. A. (2011). *Acta Cryst.* D**67**, 355–367.
Otwinowski, Z. & Minor, W. (1997). *Methods Enzymol.* **276**, 307–326.
Phillips, R. S. (1989). *J. Am. Chem. Soc.* **111**, 727–730.
Phillips, R. S., Bender, S. L., Brzovic, P. & Dunn, M. F. (1990). *Biochemistry*, **29**, 8608–8614.
Phillips, R. S., Demidkina, T. V. & Faleev, N. G. (2003). *Biochim. Biophys. Acta*, **1647**, 167–172.
Phillips, R. S., Demidkina, T. V., Zakomirdina, L. N., Bruno, S., Ronda, L. & Mozzarelli, A. (2002). *J. Biol. Chem.* **277**, 21592–21597.
Phillips, R. S. & Gollnick, P. D. (1989). *J. Biol. Chem.* **264**, 10627–10632.
Phillips, R. S., Ravichandran, K. & Von Tersch, R. L. (1989). *Enzyme Microb. Technol.* **11**, 80–83.
Suelter, C. H. & Snell, E. E. (1977). *J. Biol. Chem.* **252**, 1852–1857.
Suelter, C. H., Wang, J. & Snell, E. E. (1976*a*). *Anal. Biochem.* **76**, 221–232.
Suelter, C. H., Wang, J. & Snell, E. E. (1976*b*). *FEBS Lett.* **66**, 230–232.
Toraya, T., Nihira, T. & Fukui, S. (1976). *Eur. J. Biochem.* **69**, 411–419.
Tsesin, N., Kogan, A., Gdalevsky, G. Y., Himanen, J.-P., Cohen-Luria, R., Parola, A. H., Goldgur, Y. & Almog, O. (2007). *Acta Cryst.* D**63**, 969–974.